

# Preservation of NADH Voltammetry for Enzyme-Modified Electrodes Based on Dehydrogenase

Mark A. Hayes<sup>\*,†</sup> and Werner G. Kuhr<sup>†</sup>

Department of Chemistry and Biochemistry, Arizona State University, Tempe, Arizona 85287, and Department of Chemistry, University of California, Riverside, Riverside, California 92521

**Minimizing overpotential and generating high faradaic currents are critical issues for fast-scan voltammetry of  $\beta$ -nicotinamide adenine dinucleotide (NADH) for the sensitivity of enzyme-modified electrodes based on dehydrogenases. Although NADH voltammetry exhibits high overpotential and poor voltammetric peak shape at solid electrode surfaces, modification of the electrode surface can improve the electrochemical response at carbon fibers. However, these improvements are severely degraded upon the covalent attachment of enzyme. The creation of improved electron-transfer properties and the retention of these properties throughout the enzyme attachment process is the focus of this study. A novel polishing and electrochemical pretreatment method was developed which generated a decreased overpotential and a high faradaic current at carbon-fiber electrodes for NADH. Factors that lead to a degradation of voltammetric response during the enzyme fabrication were investigated, and both the aging and the covalent modification of the pretreated surface contributed to this degradation. Attachment processes that minimized the preparation time, in turn, maximized the retention of the facile electron-transfer properties. These attachment processes included varying the surface attachment reactions for the enzyme. Preparation time reduction techniques included modeling existing techniques and then improving kinetic and mass transport issues where possible. Alternate covalent attachment methods included a direct electrochemical amine reaction and an electrochemically reductive hydrazide reaction. The surface attachment and retention of electron-transfer properties of these probes were confirmed by fluorescence and electrochemical studies.**

Fast-scan cyclic voltammetry (FSCV) has been used in conjunction with enzyme-modified electrodes to monitor nonelectroactive species, most notably glutamate.<sup>1,2</sup> The surface of these covalently modified electrodes serve dual, competing functions: sites for electron transfer and enzyme attachment sites. A

degradation of electron-transfer properties for  $\beta$ -nicotinamide adenine dinucleotide (NADH) FSCV occurs upon modification with the enzyme, thereby decreasing sensitivity.<sup>3,4</sup> The purpose of the present study is threefold: to adapt 10- $\mu$ m carbon-fiber fabrication techniques to 32- $\mu$ m carbon-fiber electrodes, to improve the electron-transfer properties of these new electrodes, and to maximize the retention of these properties for the enzyme-modified electrodes.

The electrochemical oxidation of NADH exhibits a large overpotential at most solid electrode materials (the  $E_{1/2}$  for the electrochemical oxidation<sup>5–10</sup> is typically 0.50–0.80 V vs SCE compared to  $E^0$  calculated for the homogeneous reaction,<sup>6–11</sup> which is –0.56 V vs SCE). Many of the details of this electron-transfer process have been investigated.<sup>6,7</sup> The reaction products adsorb to the electrode surface and passivate the electrode.<sup>9,10</sup> These problems intensify in the presence of  $\text{NAD}^+$ .<sup>6</sup>

Several schemes decrease overpotential (or activate) carbon electrodes for a variety of analytes.<sup>12–38</sup> These schemes in-

<sup>†</sup> Arizona State University.

<sup>†</sup> University of California, Riverside.

(1) Pantano, P.; Kuhr, W. G. *Electroanalysis* **1995**, *7*, 405–416.

(2) Pantano, P.; Stamford, J. A.; Kuhr, W. G. *Proc. Electrochem. Soc.* **1993**, *93-2*, 776–777.

(3) Kuhr, W. G.; Barrett, V. L.; Gagnon, M. R.; Hopper, J. P.; Pantano, P. *Anal. Chem.* **1993**, *65*, 617–22.

(4) Pantano, P.; Kuhr, W. G. *Anal. Chem.* **1993**, *65*, 623–30.

(5) Blankespoor, R. I.; Miller, L. L. *J. Electroanal. Chem. Interfacial Electrochem.* **1984**, *172*, 231–41.

(6) Moiroux, J.; Elving, P. J. *Anal. Chem.* **1979**, *51*, 346–50.

(7) Moiroux, J.; Elving, P. J. *J. Am. Chem. Soc.* **1980**, *102*, 6533–38.

(8) Samec, Z.; Bresnahan, W. T.; Elving, P. J. *J. Electroanal. Chem. Interfacial Electrochem.* **1982**, *133*, 1–23.

(9) Moiroux, J.; Elving, P. J. *Anal. Chem.* **1978**, *50*, 1056–62.

(10) Cenas, N. K.; Kanapieniene, J. J.; Kuls, J. J. *J. Electroanal. Chem. Interfacial Electrochem.* **1985**, *189*, 163–69.

(11) Gorton, L.; Torstensson, A.; Jaegfeldt, H.; Johansson, G. *J. Electroanal. Chem. Interfacial Electrochem.* **1984**, *161*, 103–20.

(12) Evans, J. F.; Kuwana, T. *Anal. Chem.* **1977**, *49*, 1632.

(13) Evans, J. F.; Kuwana, T. *Anal. Chem.* **1979**, *51*, 358.

(14) Poon, M.; McCreery, R. L. *Anal. Chem.* **1986**, *58*, 2745.

(15) Poon, M.; McCreery, R. L.; Engstrom, R. C. *Anal. Chem.* **1988**, *60*, 1725.

(16) Strein, T. G.; Ewing, A. G. *Anal. Chem.* **1991**, *63*, 194.

(17) Stutts, K. J.; Kovach, P. M.; Kuhr, W. G.; Wightman, R. M. *Anal. Chem.* **1983**, *55*, 1632.

(18) Wightman, R. M.; Deakin, M. R.; Kovach, P. M.; Kuhr, W. G.; Stutts, K. J. *J. Electrochem. Soc.* **1984**, *131*, 1578.

(19) Blom, H. J.; Andersson, H. C.; Krasnewich, D. M.; Gahl, W. A. *J. Chromatogr.* **1990**, *533*, 11.

(20) McCreery, R. L.; Packard, R. T. *Anal. Chem.* **1989**, *61*, 775A.

(21) Kepley, L. J.; Bard, A. J. *Anal. Chem.* **1988**, *60*, 1459.

(22) Hu, I. F.; Karweik, D. H.; Kuwana, T. *J. Electroanal. Chem.* **1985**, *188*, 59.

(23) Wang, J.; Tuzhi, P.; Villa, V. *J. Electroanal. Chem.* **1987**, *234*, 119.

(24) Feng, J.; Brazell, M.; Renner, K.; Kasser, R.; Adams, R. N. *Anal. Chem.* **1987**, *59*, 1863.

clude radio frequency in an oxygen atmosphere,<sup>12,13,18,31,37</sup> laser irradiation,<sup>14–16,29,32,38</sup> thermal treatment,<sup>17,18,31,36</sup> and electrochemical treatment.<sup>19–28,33–35</sup> Carbon-fiber disk electrodes (10- $\mu$ m diameter) have been electrochemically pretreated for FSCV of NADH.<sup>3</sup> Activation of the electrode may be caused by removal of contaminants, alterations of surface functionalities, or modification of surface micromorphology.<sup>17,23,26,27,39–41</sup>

Exposure to environmental forces after activation of the electrode surface increases the overpotential in many systems.<sup>29,42–44</sup> The current response diminishes as much as 90% and overpotential increases during the implantation process prior to in vivo monitoring of dopamine with electrochemical probes.<sup>42</sup> In situ measurements also show an increase in overpotential which has been attributed to adsorption of airborne impurities<sup>29</sup> or through diffusion-based contamination by organic impurities.<sup>43</sup> Finally, loss of oxygen redox functionalities (e.g., the quinone–hydroquinone couple) could account for the loss of activation.<sup>44</sup>

Covalent chemical modification has been used extensively to change the properties of carbon-fiber surfaces.<sup>45,46</sup> Much of the initial work for the covalent attachment of enzymes focused on immobilization reactions that used cyanuric chloride or direct carbodiimide linkage.<sup>47,48</sup> However, these attachment schemes suffer from several drawbacks, including exposing the enzyme to pH and ionic strength flux and large potential gradients during potential sweep experiments.<sup>4</sup> An avidin–biotin attachment spacer has been used to produce an electrochemical probe for glutamate using 10- $\mu$ m-diameter carbon-fiber microelectrodes.<sup>4</sup> This avidin–biotin technology uniquely allows the separate optimization of the surface attachment reactions and the modifications to enzymes necessary to adhere them to these surface structures.

This attachment system has been characterized by electrochemical analysis and fluorescence imaging.<sup>49–51</sup> Electrochemical measurements were performed to monitor the alterations of the electron-transfer properties of the electrode by the fabrication process. Fluorescence imaging of the enzyme attachment sites used FITC-conjugated avidin during fabrication. The distribution of possible electron-transfer sites, specifically, the distribution of surface carboxylates and carbonyls, was characterized using electrochemically generated chemiluminescence.<sup>50,51</sup>

In the present study, polishing and pretreatment strategies were investigated for 32- $\mu$ m carbon-fiber electrodes. These efforts were designed to improve and preserve electron-transfer properties through the enzyme modification process. First, 32- $\mu$ m-diameter carbon-fiber electrodes were polished and electrochemically pretreated to minimize the overpotential and increase the faradaic current for the oxidation of NADH. Second, the effects of aging (either in air or in solution) were investigated and were shown to degrade the NADH electrochemical response. On the basis of this, the fabrication time for the adapted avidin–biotin tether system was minimized. The effects of temperature, diffusion, and convective mass transport were considered.

The degradation of electron-transfer properties observed for the enzyme-modified electrodes exceeded the effects due to solution aging alone. To minimize this additional source of degradation, two different surface attachment schemes were explored. One method, biotin hydrazide reduction, holds great promise for further improvements in NADH response while providing for efficiently tethered enzyme.

## EXPERIMENTAL SECTION

**Chemicals.** ExtrAvidin (avidin), NAD<sup>+</sup>, NADH, 1-ethyl-3-[(dimethylamino)propyl]carbodiimide (EDC), FITC-ExtrAvidin (FITC-avidin), glutamate, and glutamate dehydrogenase (GDH), 40 units/mg (EC 1.4.1.3, Sigma Chemical Co., St. Louis, MO), sulfo-NHS-LC-biotin (biotin) and biotin hydrazide (Pierce Chemical Co., Rockford, IL), and poly(oxyalkylene)diamine (Jeffamine ED-2001, Texaco Chemical Co., Houston, TX) were used as received. Phosphate buffer (PBS, 0.15 M NaCl, 0.10 M Na<sub>2</sub>HPO<sub>4</sub>, pH 8.5) was prepared with reagent-grade chemicals in water purified by a Milli-Q water purification system (Millipore, Bedford, MA). All FSCV measurements were conducted in pH 8.5 PBS.

**Carbon-Fiber Microelectrode Preparation.** The fabrication of carbon-fiber microelectrodes has been described previously.<sup>4</sup> Briefly, all carbon-fiber microelectrodes (32- $\mu$ m-diameter carbon fiber, Tectron Specialty Materials, Lowell, MA) were beveled at a 30° angle for 10 s to 2 min on a polishing wheel embedded with 8–10- $\mu$ m diamond particles (Sutter Glass, Novato, CA). In some instances, where noted, polishing was performed under a stream of dehydrated house air. After polishing, the electrodes were placed in pH 8.5 PBS and treated with a –0.2 to +2.0 V (50 Hz, 9 s) voltammetric waveform. The electrode was exposed to ~1000 analytical voltammetric scans (see instrumentation section) to obtain a stable background response and then tested with 100  $\mu$ M NADH under flow injection analysis (FIA) conditions. All potentials are recorded vs an Ag/AgCl reference electrode.

- (25) Gonon, F. G.; Formbarlet, C. M.; Buda, M. J.; Pujopl, J. F. *Anal. Chem.* **1981**, 53, 1386.
- (26) Engstrom, R. C. *Anal. Chem.* **1982**, 54, 2310.
- (27) Fishman, H. A.; Ewing, A. G. *Electroanalysis* **1991**, 3, 899.
- (28) Saraceno, R. A.; Ewing, A. G. *Anal. Chem.* **1988**, 60, 2016.
- (29) Rice, R. J.; Pontikos, N. M.; McCreery, R. L. *J. Am. Chem. Soc.* **1990**, 112, 4618.
- (30) Kamau, G. N.; Willis, W. S.; Rusling, J. F. *Anal. Chem.* **1985**, 57, 2759.
- (31) Fagan, D. T.; Hu, I. F.; Kuwana, T. *Anal. Chem.* **1985**, 57, 545.
- (32) Poon, M.; McCreery, R. L. *Anal. Chem.* **1987**, 59, 1615.
- (33) Engstrom, R. C.; Strasser, V. A. *Anal. Chem.* **1984**, 56, 136.
- (34) Cabaniss, G. E.; Diamantis, A. A.; Murray, W. R., Jr.; Linton, R. W.; Meyer, R. J. *J. Am. Chem. Soc.* **1985**, 107, 1845.
- (35) Falat, L.; Cheng, H. Y. *J. Electroanal. Chem.* **1983**, 157, 393.
- (36) Wightman, R. M.; Park, E. C.; Borman, S.; Dayton, M. A. *Anal. Chem.* **1978**, 50, 1410.
- (37) Miller, C. W.; Karweik, D.; Kuwana, T. *Anal. Chem.* **1979**, 53, 2319.
- (38) Poon, M.; McCreery, R. L. *Anal. Chem.* **1988**, 60, 1725.
- (39) Hu, I. F.; Kuwana, T. *Anal. Chem.* **1986**, 58, 3235.
- (40) Kovach, P. M.; Deakin, M. R.; Wightman, R. M. *J. Phys. Chem.* **1986**, 90, 4612.
- (41) Deakin, M. R.; Kovach, P. M.; Stutts, K. J.; Wightman, R. M. *Anal. Chem.* **1986**, 58, 1474–1480.
- (42) Stamford, J. A.; Crespi, F.; Marsden, C. A. In *Monitoring Neuronal Activity*; Stamford, J. A., Ed.; The Practical Approach Series; Oxford University Press: New York, 1992; pp 113–144.
- (43) McCreery, R. L. In *Electroanalytical Chemistry*; Bard, A. J., Ed.; Marcel Dekker: New York, 1978; Vol. 17, Chapter 5.
- (44) Armstrong, F. A.; Bond, A. M.; Hill, A. O.; Psaltis, I. S. M.; Zoski, C. G. *J. Phys. Chem.* **1989**, 93, 6485–6493.
- (45) Murray, R. W., Ed. *Molecular Design of Electrode Surfaces*; Techniques in Chemistry Series; John Wiley & Sons: New York, 1992.
- (46) Turner, A. P. F.; Karube, I.; Wilson, G. S. *Biosensors*; Oxford University Press: New York, 1987; p 770.
- (47) Ianiello, R. M.; Yacynych, A. M. *Anal. Chem.* **1981**, 53, 2090–2095.
- (48) Ianiello, R. M.; Lindsey, T. J.; Yacynych, A. M. *Anal. Chem.* **1982**, 54, 1980–1984.

(49) Pantano, P.; Kuhr, W. G. *Anal. Chem.* **1991**, 63, 1413–1418.

(50) Pantano, P.; Kuhr, W. G. *Anal. Chem.* **1993**, 65, 2452–2458.

(51) Hopper, P.; Kuhr, W. G. *Anal. Chem.* **1994**, 66, 1996–2004.

**Covalent Attachment of Enzyme.** The electrode was then subjected to one of the following enzyme attachment procedures.

**Fabrication Based on EDC Surface Attachment.** This procedure is based on the work of Pantano and Kuhr, but it has been extensively modified.<sup>4</sup> The rationale for the modifications are described in later sections. The electrode was pretreated and tested. It was then placed in an EDC solution (30 mg/mL pH 6.5 PBS) for 15 min at 60 °C. The EDC serves to activate the surface carboxylates to be reactive to amines.<sup>52</sup> Next, an ~100-Å diamine tether was allowed to react by placing the electrode, without rinsing, into a Jeffamine 2001 solution (86 mg/mL pH 7.4 PBS) for 15 min at 60 °C. The electrode was rinsed with water and placed in a biotin (5 mg/mL pH 7.4 PBS) solution for 15 min at room temperature to allow the remaining exposed amine to react. The biotinylated electrode was rinsed, placed in avidin (5 mg/mL), an extremely stable protein with four strong binding sites to biotin, for a minimum of 3 h, and gently rocked. The electrodes were then exposed to a solution of biotinylated-GDH and gently rocked (GDH was biotinylated by a standard procedure<sup>4</sup>) for a minimum of 12 h at 38 °C.

**Surface Attachment via Oxidative Amination.** Electrochemically pretreated electrodes were placed in 0.1 M tetrabutylammonium perchlorate in acetonitrile solution containing 86 mg/mL Jeffamine 2001. Three cyclic voltammogram waveforms of 0–1.5 V (10 mV/s) were applied to the electrode in this solution. The current caused by the attachment reaction, if present, was undetected within the background current. Next, the electrodes were exposed to the biotin, avidin (or FITC-avidin), and biotinylated-GDH solutions as described above.

**Reductive Hydrazide Surface Attachment.** The pretreated electrode was placed in a pH 8.5 phosphate buffer containing 3 mg/mL biotin hydrazide, and three cyclic voltammetric waveforms of 0 to –1.4 V (10 mV/s) were applied. Again, the current caused by the attachment reaction, if present, was undetected. The electrode was then exposed to avidin (or FITC-avidin) and biotinylated-GDH solutions as described above.

**Instrumentation.** The rationale for and description of data acquisition and manipulation equipment has been presented elsewhere.<sup>4</sup> Briefly, fast-scan cyclic staircase voltammetry in a FIA system was performed via a computer-controlled EI-400 potentiostat (Ensman Instruments, Bloomington, IN) with the working electrode preamplifier placed inside a faraday cage. The analytical voltammetric waveform was from 0 to 1.1 V at 100 V/s every 200 ms. Data were collected from the potentiostat through a 12-bit A/D (Labmaster DMA, Scientific Solutions, Solon, OH) to a 80486-PC for data analysis and manipulation with DOS- and Windows-based software written in-house.<sup>53</sup> This software allowed the data to be represented as cyclic voltammograms, background-subtracted cyclic voltammograms (to obtain  $E_p$ , peak potential, and  $i_p$ , peak current), background-subtracted average current vs time plots ( $i_{av}$  vs  $t$ ), or average current vs time plots. The rationale and optimization of background-subtraction voltammetry have been presented elsewhere.<sup>53</sup> Briefly, nonfaradaic currents arising from ionic strength and pH flux are considered constant throughout the voltammetric scan range. Nonfaradaic current response in potential ranges without oxidative NADH current may be used

to normalize the current within the oxidative current potential range.<sup>53</sup> The current between 200 and 400 mV was subtracted from the current between 600 and 1100 mV in each voltammogram to obtain plots of average background-subtracted current vs time. The first derivative data of the cyclic voltammograms were calculated with a document written in-house with MathCAD 5.0+ (MathSoft Inc., Cambridge, MA). All errors are reported as standard error of the mean (SEM).

**Fluorescence Microscopy.** The fluorescence imaging system has been described previously.<sup>49–51</sup> The system consisted of a Carl Zeiss Axioplan microscope equipped with a 200-W mercury arc lamp for illumination in the epifluorescent configuration. Filters were used for FITC at 488-nm excitation and 519-nm emission. Images were obtained through a Epiplan Neofluar 40× water immersion lens. Digital images were obtained with a Peltier-cooled, Thompson 7895B CCD (class 2, 512 × 512, Metachrome II UV-coated, MPP mode) which was operated at –45 °C through a Photometrics NU-200 controller (16-bit, 40-kHz A/D; MacIntosh IICI configuration). Data collection was controlled by IP-LAB 2.3.0.C software (Signal Analytics, Vienna, VA). Subsequent data processing was performed on IP-LAB, NIH image 1.40 (Public Domain, Wayne Rasband) and/or Spyglass Transform 3.1 (Spyglass, Inc., Champaign, IL). White light illumination from an arc lamp was used (after its intensity was reduced by two consecutive 1% transmitting neutral density filters) to image the physical features of the carbon surface and to delineate the exact area of the polished carbon surface (to avoid the inclusion of surrounding epoxy and glass in the analysis). Exposure time and gain factors were 0.5 s and 10, respectively, for all fluorescence images. Histograms of fluorescence signal intensity vs frequency of occurrence were used to assess the fluorescent signal from the electrode surface.

## RESULTS AND DISCUSSION

Enzyme-modified amperometric sensors based on dehydrogenases exhibit high overpotential and low faradaic currents for FSCV of NADH at solid electrodes.<sup>1,2,4</sup> The first factor that affects the overall sensitivity for the enzyme-generated signal is the initial electrochemical response to NADH at the unmodified carbon surface. A finite amount of signal degradation occurs due to the fabrication of these sensors; therefore, maximizing the initial response provides the most sensitive post-enzyme-modified response. As the modification process is improved to reduce its deleterious effects on NADH voltammetry, this maximum response may be retained.

**Polishing and Electrochemical Pretreatment.** The initial response was improved by polishing the electrode under a dehydrated air-flow stream (<10% humidity; in conjunction with the electrochemical treatment described below). Under these conditions,  $E_p$  does not significantly change ( $783 \pm 11$  vs  $804 \pm 18$  mV) compared to controls (unaltered room humidity), but the current doubled both in terms of  $i_p$  and  $i_{av}$  vs  $t$ . The magnitude of  $i_p$  improved from  $7.71 \pm 1.81$  to  $14.60 \pm 2.03$  nA and  $i_{av}$  vs  $t$  improved from  $6.47 \pm 1.17$  to  $13.50 \pm 2.03$  nA.

In addition to polishing, the electrochemical pretreatment generated pronounced improvements in the voltammetric behavior of these probes. Figure 1A shows a background-subtracted fast-scan cyclic voltammogram obtained for 100  $\mu$ M NADH at a freshly polished carbon-fiber electrode. The initial and switching potentials

(52) Hoare, D. G.; Koshland, D. E., Jr. *J. Biol. Chem.* **1967**, *242*, 2447–2453.

(53) Hayes, M. A.; Kristensen, E.; Kuhr, W. G. *Biosens. Bioelectron.* **1998**, *13*, 1297–1305.



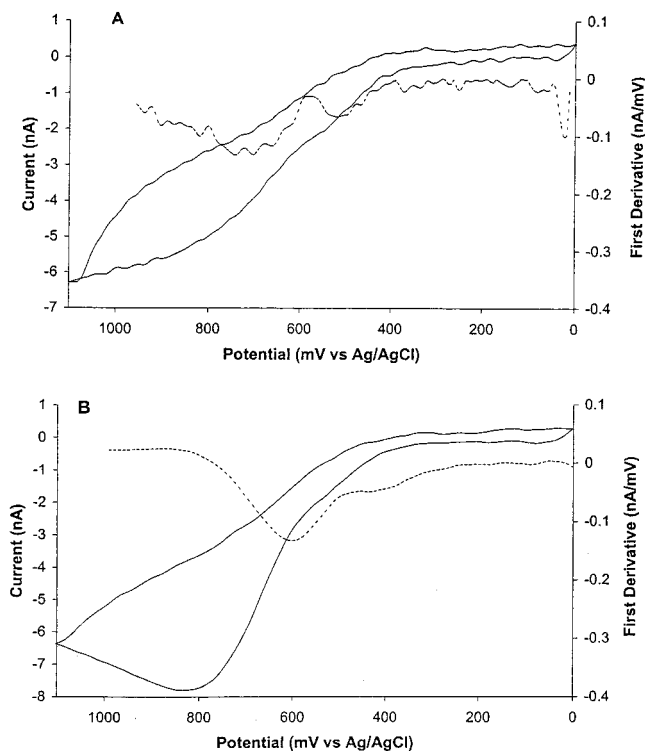


Figure 1. Fast-scan cyclic voltammogram current (—) response of 100  $\mu$ M NADH at polished (nondehumidified) 32- $\mu$ m-diameter carbon-fiber disk electrode with first derivative (---) of forward scan also plotted. Note separate scales for each. (A) is from a freshly polished electrode, and (B) is from an electrode after electrochemical pretreatment (see text).

are limited by the reduction of surface quinones and oxidation of the electrolyte, respectively.<sup>53</sup> For NADH voltammetry at untreated carbon-fiber electrodes, the  $E_p$  is greater than 1100 mV (the switching potential), and by definition,  $i_p$  is not observed in the available voltage scan range. This cyclic voltammogram demonstrates the severe overpotential that commonly exists at these carbon-fiber electrodes.

An electrochemical pretreatment in PBS, pH 8.5 (−0.2 to +2.0 V, 50 Hz, 9 s) produced the response shown in Figure 1B. In addition to the oxidative electrochemical pretreatment to 2.0 V, each electrode was cycled through  $\sim$ 1000 analytical voltammetric scans before the first NADH injection to produce stable background currents needed to generate the background-subtracted cyclic voltammograms.<sup>53</sup>

Table 1 is a summary of the voltammetric behavior of six freshly polished electrodes before and after this electrochemical pretreatment. As can be seen from the representative data from electrodes in Figure 1A and B and the compilation of the data from all six electrodes in Table 1, the electrode response is dramatically improved in regard to  $E_p$  and  $i_{av}$  vs  $t$  response. The peak potential became identifiable and was  $804 \pm 18$  mV and  $i_p$  also became defined and was  $7.71 \pm 1.81$  nA. This decrease in overpotential has a sensitivity advantage when the  $i_{av}$  vs  $t$  FIA data was assessed. The improvement in background-subtracted current (current from 600 to 1100 mV minus current from 200 to 400 mV)<sup>53</sup> vs time from these plots is +77%. Surprisingly, the  $i_p$  response (when comparing current at 1100 mV for pretreatment and  $i_p$  for posttreatment) from the cyclic voltammetry data does

Table 1. Electrochemical Behavior of NADH Before and After Electrochemical Treatment

electrochem parameter	treatment <sup>a</sup>		% change
	preelectrochem	postelectrochem	
$E_p$ (mV)	>1100	$804 \pm 16$	
$i_p$ (nA)	$6.83 \pm 1.47^b$	$7.71 \pm 1.81$	
$i_{ave}$ vs $t$ (nA) <sup>c</sup>	$3.65 \pm 0.97$	$6.47 \pm 1.17$	+77
$(di/dE)_{mag}$ (nA/mV)	$0.07 \pm 0.02$	$0.13 \pm 0.01$	+84

<sup>a</sup> All errors quoted are SEM. <sup>b</sup>  $i_p$  for pretreatment data simply taken at switching potential. <sup>c</sup> Average current from 600 to 1100 mV minus average current from 200 to 400 mV vs time for a 4-s FIA injection of 100  $\mu$ M NADH.

not differ;  $6.83 \pm 1.47$  and  $7.71 \pm 1.81$  nA. This seeming inconsistency can be understood by realizing that the background-subtracted current is integrated from 600 to 1100 mV. While the current magnitude of any one region is not greater than the current at 1100 mV for pretreatment, the integrated current has significantly increased.

In addition to monitoring  $E_p$  and  $i_p$  to assess electron-transfer properties, the first derivative of the forward scan of the cyclic voltammogram was calculated, yielding both the magnitude  $[(di/dE)_{mag}]$  and position of maximum slope. The first, second, and third derivatives of the current for irreversible systems have been explored for improved data analysis.<sup>54,55</sup> The need for additional descriptive information for NADH voltammetry is illustrated in Figure 2. The difference between the voltammograms in A and B is poorly described by simply stating that the voltammetry became somewhat less reversible and  $E_p$  either became more difficult to discern or shifted out of the voltammetric scan range. Clearly, much of the current generated in the 600–800 mV range in Figure 2A is still present in Figure 2B and contributes to sensitivity in  $i_{av}$  vs  $t$  analysis. The first-derivative analysis technique is of greater value for evaluating differences between moderately and severely degraded voltammetry. Examples of this degraded voltammetry evaluation will be discussed in the context of the alternate attachment schemes (see below).

The effect of dehydrated polishing could be quantitated with conventional measures. This provides a method to compare the relative response of the first-derivative data with the standard parameters. The position of the maximum slope remained constant,  $663 \pm 9.6$  and  $673 \pm 18$  mV, and  $[(di/dE)_{mag}]$  increased from  $0.13 \pm 0.01$  to  $0.31 \pm 0.05$  nA/mV. Thus, the information available from the first derivative reflects qualities similar to these conventional measures.

**Electrode Aging.** Once the voltammetry for NADH at fresh carbon-fiber electrodes was optimized, it was possible to evaluate the cause of the diminished quality of voltammetry upon enzyme modification. Electrode aging alone, where the electrode response decays with time upon exposure to air or solution, dramatically affects the electrode response. To quantitatively test the aging

(54) Perone, S. P.; Evins, C. V. *Anal. Chem.* **1965**, *37*, 1061–1063.

(55) Perone, S. P.; Evins, C. V. *Anal. Chem.* **1965**, *37*, 1644–1646.

(56) Deinhammer, R. S.; Ho, M.; Anderegg, J. W.; Porter, M. D. *Langmuir* **1994**, *10*, 1306–1313.

(57) Delamar, M.; Hitmi, R.; Dinson, J.; Saveant, J. M. *J. Am. Chem. Soc.* **1992**, *114*, 5883–5884.

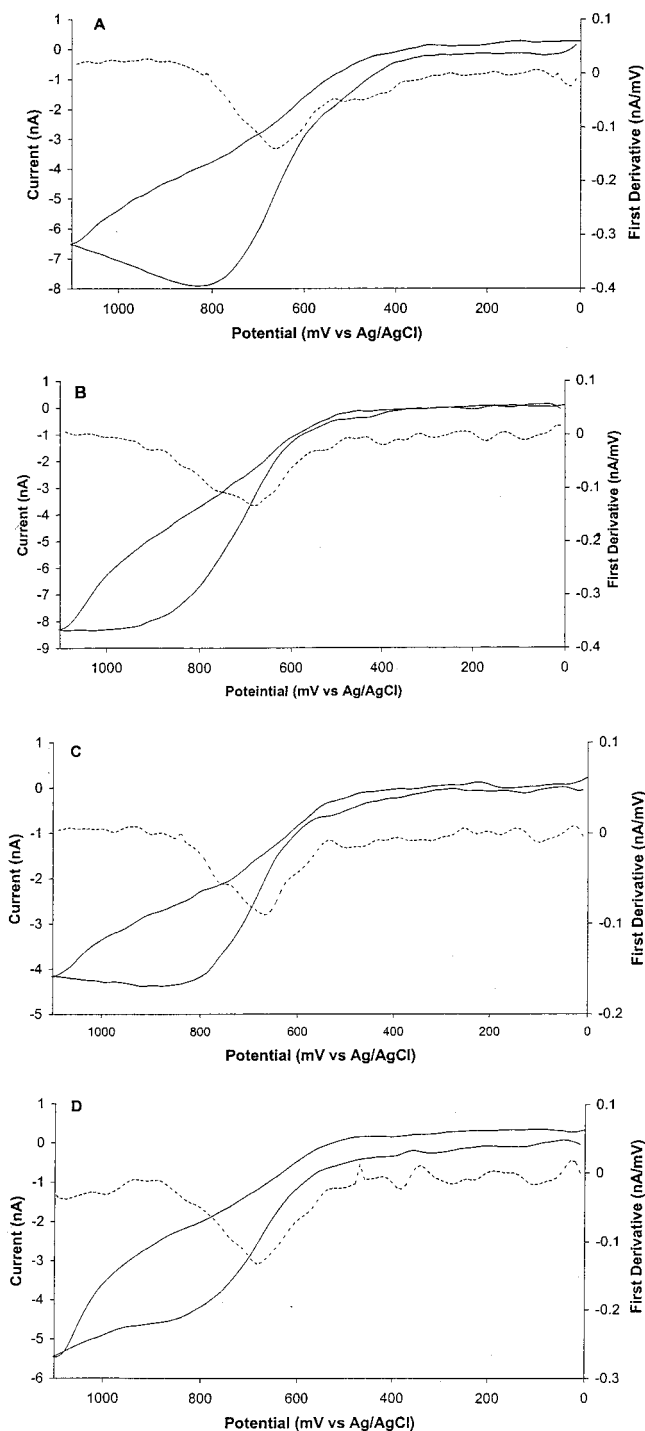


Figure 2. Fast-scan cyclic voltammogram current (—) response of 100  $\mu\text{M}$  NADH from electrochemically pretreated 32- $\mu\text{m}$ -diameter carbon-fiber disk electrode with calculated first derivative (---) of forward scan plotted. Note separate scales for each. Scans A and C are electrodes that were freshly electrochemically pretreated; scans from the same electrodes after storage in (B) PBS solution and (D) air for 4 days.

phenomena, eight electrodes were electrochemically pretreated, tested for NADH response, and then stored for 4 days (Figure 2, Table 2). Four electrodes were stored in PBS (Figure 2B) and four in air (Figure 2D). The first derivative of the forward scan was calculated (Figure 2). For all eight electrodes (Table 2), the  $E_p$  became unidentifiable at greater than 1100 mV, and therefore,

Table 2. Solution and Air-Aging Voltammetric Characteristics

electrochem parameter ( $n = 4$ )	control <sup>a</sup>	postaging <sup>a</sup>	% change
$E_p$ (mV)			
soln	864 $\pm$ 17	> 1100	
air	829 $\pm$ 20	> 1100	
$i_p$ (nA)			
soln	6.2 $\pm$ 0.6	4.5 $\pm$ 0.43 <sup>b</sup>	-27
air	4.9 $\pm$ 1.2	4.7 $\pm$ 1.3 <sup>b</sup>	
$i_{av}$ vs $t$ (nA) <sup>c</sup>			
soln	6.04 $\pm$ 1.14	4.55 $\pm$ 1.39	
air	4.10 $\pm$ 0.92	3.42 $\pm$ 0.95	
( $di/dE$ ) <sub>mag</sub> (nA/mV)			
soln	0.22 $\pm$ 0.02	0.12 $\pm$ 0.02	-44
air	0.19 $\pm$ 0.04	0.14 $\pm$ 0.03	

<sup>a</sup> All errors quoted are SEM. <sup>b</sup>  $i_p$  for post-aging data taken at switching potential. <sup>c</sup> Average current from 600 to 1100 mV minus average current from 200 to 400 mV vs time for a 4 s FIA injection of 100- $\mu\text{M}$  NADH.

Table 3. Electrochemical Behavior of NADH before and after Enzyme Modification

electrochem parameter ( $n = 8$ )	control <sup>a</sup>	postenzyme modified <sup>a</sup>	% change
$E_p$ (mV)	857 $\pm$ 36	> 1100	
$i_p$ (nA)	7.5 $\pm$ 0.8	2.7 $\pm$ 0.5 <sup>b</sup>	-64
$i_{av}$ vs $t$ (nA) <sup>c</sup>	6.2 $\pm$ 0.8	2.2 $\pm$ 0.1	-65
( $di/dE$ ) <sub>mag</sub> (nA/mV)	0.15 $\pm$ 0.02	0.049 $\pm$ 0.0032	-68

<sup>a</sup> All errors quoted are SEM. <sup>b</sup>  $i_p$  for postmodified data taken at switching potential. <sup>c</sup> Average current from 600 to 1100 mV minus average current from 200 to 400 mV vs time for a 4 s FIA injection of 100  $\mu\text{M}$  NADH.

$i_p$  became undefined. An examination of the oxidative current may still be relevant by comparing current at the switching potential (which does not correspond to  $i_p$ ) to  $i_p$  (before aging). The oxidative current decreased for all electrodes (Table 2). The first derivative of these cyclic voltammograms presented some interesting results. Surprisingly, the potential at which the maximum slope occurs remained essentially constant for both sets (688  $\pm$  5 vs 706  $\pm$  11 and 682  $\pm$  20 vs 685  $\pm$  16, solution and air, respectively) even though the voltammetry became somewhat less reversible, either making  $E_p$  more difficult to discern or increasing it at least 250 mV.

These results indicate that the carbon surface changes significantly during aging. This change could result in a complete loss of facile electron-transfer sites which leads to a shift from a linear diffusion regime to a microscopic spherical diffusion regime,<sup>44</sup> or it may result in an array of electron-transfer sites of varying energetics.<sup>41</sup> Although data from electrogenerated chemiluminescence at these surfaces is supportive of a complete loss of facile electron-transfer sites, the small size of these probes and the alteration of the wave shape makes a shift in diffusion regimes an unlikely explanation.<sup>44,50</sup>

The voltammetry of NADH was examined before and after the EDC-based derivatization process (Table 3). The results showed greater deterioration in the voltammetric signal upon modification with the enzyme and tether system than did solution- or air-aging

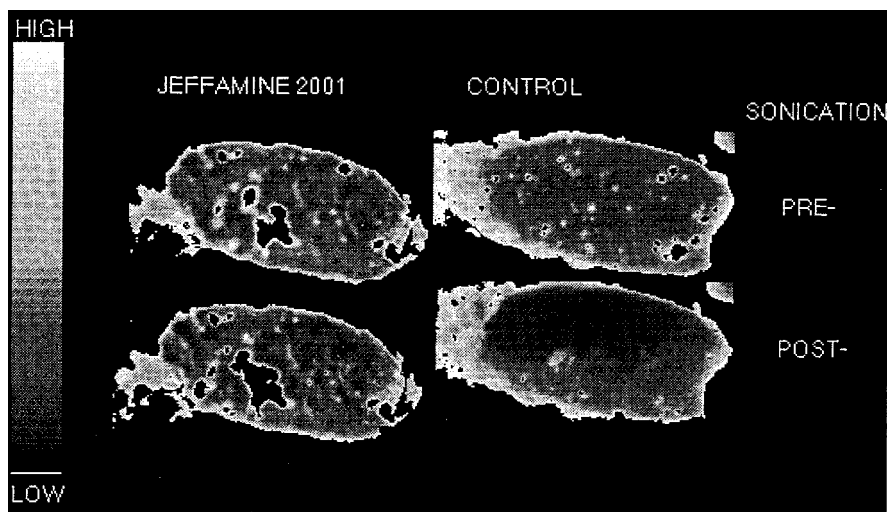


Figure 3. Fluorescence microscopy image of 32- $\mu\text{m}$ -diameter carbon-fiber electrode covalently modified with FITC-avidin attached via the amine oxidation reaction scheme. (Left side) Jeffamine present in CV buffer (see Experimental Section); (right side) amine absent; (top to bottom) before and after sonication, respectively.

alone. The overpotential was increased, but a quantitative description was not possible since the  $E_p$  becomes undefined. Several parameters indicated a decreased voltammetric quality:  $i_p$  (as defined above) decreased by 64% and  $i_{av}$  vs  $t$  decreased by 68%. While some of this change was caused by aging phenomena, there was a significant effect from the derivatization of the surface, possibly caused by steric hindrance, site of attachment, or surface contamination. Therefore, the covalent modification process was altered to, first, minimize the overall preparation time, and, second, explore alternate means of attachment to address both the aging and attachment reaction issues.

Adapting and improving the avidin–biotin method of electrode preparation was addressed. The avidin–biotin tether for carbon-fiber microelectrodes with GDH has been described in detail.<sup>4</sup> For clarity of this discussion, it will be briefly reiterated. Carboxylates on the carbon surface were activated for reaction with amines with EDC.<sup>52</sup> Jeffamine, serving as a tether of  $\sim 100$  Å, was then allowed to react with the activated carboxylates. Biotin was reacted with the free amine end of the surface-bound Jeffamine. Next, this “biotinylated surface” was exposed to avidin, which was finally allowed to bind biotinylated-GDH, thus forming an enzyme-modified electrode.

Approximate calculations indicate that a monolayer of reactant can diffuse to the electrode surface in a matter of seconds to minutes for each step. In addition, convective mass transport and increased temperature were utilized to further minimize the fabrication time. EDC and Jeffamine are stable to increased temperatures and may be exposed to higher temperatures during this process. This temperature increase has only a moderate effect on the reaction time. However, the stability of biotin, avidin (FITC-avidin), and biotinylated-GDH at elevated temperatures may present some problems, precluding this approach to improved mass-transfer and reaction kinetics. Nevertheless, convective mixing may be used to enhance the rate of mass transfer for these steps. Consequently, the temperature was raised for the EDC and Jeffamine reaction steps and convective mixing was used to accelerate the avidin and the biotinylated-GDH steps, allowing a reduction in time for all steps. The new procedure produced 32-

$\mu\text{m}$  carbon-fiber electrodes with a biotinylated surface which retains facile electron-transfer properties while decreasing preparation (and aging) time (to the avidin step) from 9 h to 45 min compared to the previously described procedure.<sup>4</sup>

**Alternative Surface Attachment Reactions.** Alternate strategies for enzyme attachment were also explored: the direct oxidative attachment of Jeffamine in a nonaqueous solution and the direct reduction of a hydrazide-containing biotin. Both strategies decreased further aging and allowed alternative surface attachment sites, possibly retaining more of the favorable electron-transfer properties attained during the pretreatment.

First, the direct electrochemical attachment of amines was performed via the protocols developed in Porter's group.<sup>56</sup> The current during amine oxidation could not be discerned from background (e.g., for monolayer coverage, one would expect to see a current of  $\sim 10$  pA). Therefore, the coverage for Jeffamine-modified electrodes was quantitated by subsequent reaction of the surface-bound Jeffamine with biotin, then by FITC-avidin conjugate, and imaging with fluorescence microscopy. A sample of a fluorescence image for this amine oxidation attachment scheme and a control (amine absent during oxidative scan) are shown in Figure 3.

As a simple test for stability of the covalently bound Jeffamine–biotin–avidin, both electrodes were sonicated. The two images prior to sonication (at the top of Figure 3) show a considerable amount of fluorescence. Apparently, some of the FITC-avidin was physisorbed to the control electrode. This material was easily removed by 20-s sonication in water, as shown in the lower portion of Figure 3. These data indicate that covalently attached Jeffamine–biotin–FITC-avidin was stable to sonication. In contrast, materials that are simply physisorbed are removed.

The digital fluorescence microscopy image of the polished fiber surface was examined quantitatively. Visual inspection of these images indicates that there are consistent very-high-intensity spots along with a general “cloudiness” apparent on all derivatized electrodes, which is absent on the control electrodes. This cloudiness had a unique characteristic in that it represented the greatest number of pixels of a given fluorescence intensity. To

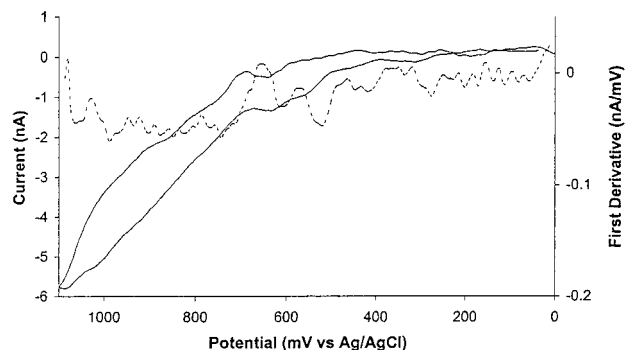


Figure 4. Representative fast-scan cyclic voltammogram current response (—) for 100  $\mu$ M NADH for 32- $\mu$ m-diameter carbon-fiber electrode immediately after the Jeffamine oxidation reaction scheme. The first derivative of the current (---) of the forward scan is also included for comparison with other data sets (note separate scale).

quantitate this effect, the number of pixels with a particular fluorescence intensity was plotted vs that intensity to generate a histogram of the image (frequency of occurrence vs fluorescence intensity). Derivatized electrodes exhibited a maximum frequency of occurrence at higher fluorescence intensity. For six Jeffamine-modified electrodes (with subsequent biotin and FITC-avidin fabrication steps for imaging), a maximum frequency of occurrence was at significantly higher intensity than controls ( $1.02 \pm 0.23 \times 10^4$  vs  $6.9 \pm 0.6 \times 10^3$ , respectively).

The same Jeffamine-modified electrodes were further characterized electrochemically. The FSCV response with first derivative plotted is shown for 100  $\mu$ M NADH of an electrode immediately after preparation (Figure 4). The electrode showed very sluggish electron-transfer properties. Quantitation of these properties for three similarly fabricated electrodes resulted in an  $E_p$  of  $>1100$  mV,  $i_p$  ( $i$  at 1100 mV) of  $4.8 \pm 1.0$  nA, the maximum slope of the current at  $942 \pm 53$  mV, and  $(di/dE)_{\text{mag}}$  of  $0.054 \pm 0.015$  nA/mV. Although the reaction produced substantial covalent attachment, the electron-transfer properties of these probes was greatly diminished.

Comparison of Figure 2B with Figure 4 illustrates the utility of quantitating between moderately and severely degraded voltammograms with the first derivative. These voltammograms cannot be evaluated by assessing standard thermodynamic or kinetic parameters and yet the voltammograms from Figure 2B and Figure 4 are strikingly different. Calculation of the first derivative allows the comparison of cyclic voltammograms when  $E_p$  (and therefore  $i_p$ ) does not occur within the available scan range. Subtleties in the cyclic voltammogram shape commonly used in describing voltammetric quality<sup>44</sup> ("good" and "bad" voltammetry) may be clearly defined. The magnitude of the maximum slope and its position shift upon electrochemical pretreatment (Table 1). The presence of a steep slope at lower potentials is directly reflected in the increased sensitivity for  $i_{\text{av}}$  vs  $t$  since more current is present in the 600–1100-mV range (Table 1). The quality of the electrode can be assessed quantitatively using the calculated first derivative but cannot be assessed with the standard electrochemical parameters, since  $i_p$  and  $E_p$  are not defined in one case.

In contrast to the amine attachment scheme, FSCV measurements of NADH immediately following the reductive hydrazide

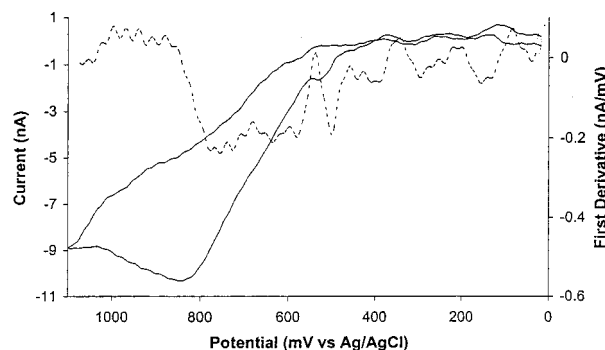


Figure 5. Representative fast-scan cyclic voltammogram current response (—) and first derivative (---) for 100  $\mu$ M NADH for 32- $\mu$ m-diameter carbon-fiber electrode immediately after the biotin hydrazide reduction reaction scheme (note separate scales).

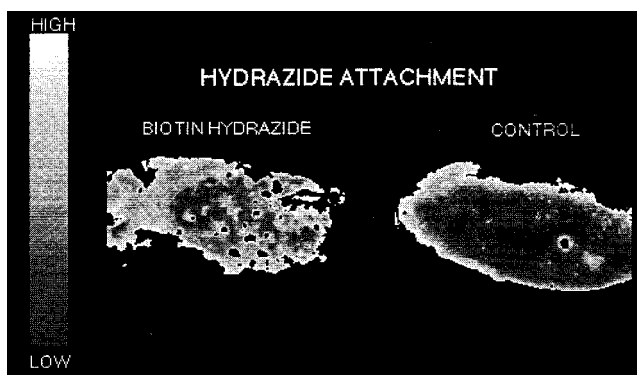


Figure 6. Fluorescence microscopy image of 32- $\mu$ m-diameter carbon-fiber electrode covalently modified with FITC-avidin attached via the biotin hydrazide reduction reaction scheme.

attachment reaction resulted in an  $E_p$  of  $840 \pm 35$  mV,  $i_p$  of  $7.6 \pm 2.5$  nA, and  $(di/dE)_{\text{mag}}$  of  $0.17 \pm 0.05$  nA/mV (Figure 5). These values are all within the experimental error of the fresh electrochemically pretreated (conventional polishing) electrodes. Thus, these values indicate an 100% retention of "good" electron-transfer properties at a fully derivatized electrochemical probe.

The efficacy of the second attachment scheme, based on biotin hydrazide reduction, was also examined using fluorescence microscopy (Figure 6). To observe attachment, the biotin-modified electrode was exposed to FITC-avidin solution and imaged. The maximum frequency of occurrence for fluorescence intensity for six hydrazide-exposed electrodes was  $8.7 \pm 0.8 \times 10^3$ , whereas the control was  $7.0 \times 10^3$ . This scheme may form a carbon lattice–nitrogen bond similar to the diazonium salt reaction mechanism. However, the attachment site and mechanism are unknown.<sup>57</sup> Two separate observations suggest that the attachment site is not the carbonyl functionality on the carbon-fiber surface, as would be the case for nonpotential bias-reaction conditions (0.0 V or uncontrolled potential) with hydrazide. First, the cyclic voltammograms generated from these surfaces indicate retention of high-quality postmodification voltammetry (Figure 5 and quantitation presented above). The retention of this voltammetry does not occur for the nonpotential bias exposure to the hydrazide solution (data not shown). Therefore, the site of attachment presumably is different. Second, in separate fluorescence and electrogenerated chemiluminescence<sup>50</sup> studies, the electron-transfer site appears to be the surface oxide carbonyl, and the attachment to this

functional group precluded facile voltammetry. This attachment scheme appears promising. Consequently, quantitating the amount of enzyme loaded onto the surface and optimization of the reaction conditions are the focus of future investigations.

#### CONCLUSION

The retention of facile electron-transfer properties for NADH at modified carbon-fiber electrodes was maximized by adapting and improving the previous carbon-fiber fabrication process. This was confirmed by electrochemical evidence showing that decreased manufacture time and alternative covalent attachment schemes could retain favorable properties. Fluorescence microscopy independently confirmed the presence of the surface

modifications while retaining the favorable electrochemical properties.

#### ACKNOWLEDGMENT

This work was supported by, in part, by the National Institutes of Health (Grant GM44112-01A1) and a Presidential Young Investigator Award (W.G.K.) from the National Science Foundation (Grant CHE 8957394). M.A.H. is a National Institutes of Health NRSA recipient (Grant 1 F32 NS09729-01).

Received for review March 30, 1998. Accepted February 11, 1999.

AC980354X